Available online at www.sciencedirect.com
ScienceDirect
Journal of Solid State Chemistry 180 (2007) 1846–1851
JOURNAL OF SOLID STATE CHEMISTRY
www.elsevier.com/locate/jssc

Crystal structure of $Ln_{1/3}NbO_3$ (Ln = Nd, Pr) and phase transition in $Nd_{1/3}NbO_3$

Zhaoming Zhang[a,*], Christopher J. Howard[a], Brendan J. Kennedy[b], Kevin S. Knight[c], Qingdi Zhou[b]

[a]*Australian Nuclear Science and Technology Organisation, Private Mail Bag 1, Menai, NSW 2234, Australia*
[b]*School of Chemistry, University of Sydney, Sydney, NSW 2006, Australia*
[c]*ISIS Facility, Rutherford Appleton Laboratory, Chilton, Didcot, OX11 0QX, UK*

Received 6 February 2007; received in revised form 20 March 2007; accepted 22 March 2007
Available online 12 April 2007

Abstract

The crystal structure of the *A*-site deficient perovskite $Ln_{1/3}NbO_3$ (Ln = Nd, Pr) at room temperature has been determined, for the first time, as orthorhombic in space group *Cmmm* using high-resolution neutron powder diffraction. Pertinent features are the alternation of unoccupied layers of *A*-sites and layers partly occupied by *Ln* cations, as well as out-of-phase tilting of the NbO_6 octahedra around an axis perpendicular to the direction of the cation/vacancy ordering. The phase transition behaviour of $Nd_{1/3}NbO_3$ has also been studied in situ. This compound undergoes a continuous phase transition at around 650 °C to a tetragonal structure in space group *P*4/*mmm* due to the disappearance of the octahedral tilting. The analysis of spontaneous strains shows that this phase transition is tricritical in nature.

Keywords: Perovskites; Crystal structures; Octahedral tilting; Cation/vacancy ordering; Phase transition; Neutron powder diffraction

1. Introduction

There has been a great deal of interest in the *A*-site deficient perovskites such as $Ln_{1/3}NbO_3$ (Ln = La, Ce, Pr, Nd), due to the promising potential of these materials as host crystals for Li^+-ion intercalation [1,2] as well as their interesting electrical properties [3–5]. The crystal structure of the $Ln_{1/3}NbO_3$ (Ln = La, Ce, Pr, Nd) compounds was first reported by Iyer and Smith 40 years ago [6]. Although their Guinier patterns showed small orthorhombic splitting, the structures of $Ln_{1/3}NbO_3$ (Ln = La, Ce, Pr, Nd) were all refined as tetragonal in space group *P*4/*mmm* on a $1 \times 1 \times 2$ cell (referred to the edge of the cubic perovskite aristotype). The doubling of the *c*-parameter was a result of *A*-site cation/vacancy ordering onto alternate (001) planes. Later Abakumov et al. reported that the symmetry for $Ln_{1/3}NbO_3$ (Ln = La, Ce, Nd) was orthorhombic in space group *Pmmm* (also on a $1 \times 1 \times 2$ cell) [4], whereas Bridges et al. determined the structure of $Ce_{1/3}NbO_3$ as monoclinic in *P*2/*m* [7]. More recently a different space group of *Cmmm* (on a $2 \times 2 \times 2$ cell) was proposed for $La_{1/3}NbO_3$ [8–10]. This was supported by Howard and Zhang using group theoretical analysis [11]. They concluded that the correct structural model for $La_{1/3}NbO_3$ is orthorhombic in *Cmmm* — the same as for $La_{2/3}TiO_3$, and identified the orthorhombic distortion as a consequence of the cation/vacancy ordering combined with out-of-phase octahedral tilting around an axis perpendicular to the ordering direction. It was also suggested by these authors, based on literature data, that the same structure may be adopted by all $Ln_{2/3}TiO_3$, $Ln_{1/3}NbO_3$ and $Ln_{1/3}TaO_3$ (Ln = La, Ce, Pr, Nd) compounds (e.g., they demonstrated that the reported monoclinic structure of $Ce_{1/3}NbO_3$ in *P*2/*m* [7] could be described equally well using the orthorhombic model in *Cmmm*). However, a recent study of $Nd_{0.7}Ti_{0.9}Al_{0.1}O_3$ (believed to be isostructural to $Nd_{2/3}TiO_3$) revealed its room temperature structure as monoclinic in space

*Corresponding author. Fax: +61 2 9543 7179.
E-mail address: zhaoming.zhang@ansto.gov.au (Z. Zhang).

0022-4596/$ - see front matter © 2007 Elsevier Inc. All rights reserved.
doi:10.1016/j.jssc.2007.03.029

group $C2/m$ on a $2\times2\times2$ cell; the lower symmetry was attributed to the smaller ionic radius[1] of Nd^{3+} (1.27 Å) than La^{3+} (1.36 Å) [13]. This monoclinic structure is characterised by A-site cation/vacancy ordering along the c-axis and out-of-phase TiO_6 octahedral tilting independently around c- and a-axis (these being parallel and perpendicular to the ordering direction, respectively).

The main aim of the present study is to examine the structure of $Ln_{1/3}NbO_3$ ($Ln=$ Nd and Pr) at room temperature, to establish whether the smaller (than La) A-site cation also results in lower symmetry than that for $La_{1/3}NbO_3$. Temperature dependent studies were also carried out to determine whether heating removes octahedral tilting as observed for $La_{1/3}NbO_3$.

2. Experimental

The polycrystalline samples of $Nd_{1/3}NbO_3$ and $Pr_{1/3}NbO_3$ were prepared by standard high-temperature ceramic methods. Nd_2O_3 (99.9% in purity, Aldrich) and Pr_6O_{11} (99.9%, Aldrich) starting powders were first preheated at 1000 °C overnight, and then mixed with Nb_2O_5 (99.9%, Aldrich) in an agate mortar under acetone. The mixtures were subsequently placed in alumina crucibles and heated at temperatures of 800 °C for 20 h and 1300 °C for 50 h with intermediate grinding. The sample purity was confirmed by powder X-ray diffraction measurements using a Shimadzu D-6000 diffractometer with Cu$K\alpha$ radiation.

Time-of-flight powder neutron diffraction data were recorded using the high-resolution powder diffractometer, HRPD, at the ISIS neutron facility, Rutherford Appleton Laboratories, UK [14]. The powdered samples of $Nd_{1/3}NbO_3$ and $Pr_{1/3}NbO_3$ were loaded into thin-walled 11 mm diameter vanadium sample cans, which were then suspended from the standard ISIS candlesticks for room temperature measurements. Temperature dependent studies were also carried out for $Nd_{1/3}NbO_3$, from 100 to 750 °C. For these measurements, the vanadium sample can was mounted in an ISIS designed furnace. This furnace employs a cylindrical vanadium element and operates under high vacuum (pressure $<10^{-4}$ mbar). The thermometry is based on type-K (chromel-alumel) thermocouples positioned in contact with the sample can at about 20 mm above the beam centre. During data collection in furnace, the temperature fluctuation is approximately ±0.5 °C. The diffraction patterns were recorded over the time-of-flight range 30–130 ms in both back-scattering and 90° detector banks, corresponding to d-spacings from 0.6 to 2.6 Å (at a resolution $\Delta d/d\sim4\times10^{-4}$) and from 0.9 to 3.7 Å ($\Delta d/d\sim2\times10^{-3}$), respectively. The patterns were normalised to the incident beam spectrum as recorded in the upstream monitor, and corrected for detector efficiency according to prior calibration with a vanadium scan. Patterns were recorded to a total incident proton beam of at least 70 μA h at room temperature, corresponding to approximately 2.2 h of data collection, to allow precise structure determination. The high-temperature patterns were recorded to a total incident proton beam of about 8 μA h, corresponding to roughly 15 min of data collection, sufficient to give a good determination of lattice parameters and reasonable estimates of internal co-ordinates. The temperature intervals were typically 20 °C, but varied from 10 to 50 °C. In order to allow for thermal equilibration of the sample, data collection was delayed for a period of at least 5 min (depending on the size of the temperature step) after stability at the set temperature had been achieved.

[1]The ionic radii of Ln^{3+} quoted in this paper are those in 12-fold coordination as published by Shannon [12].

3. Results and discussion

3.1. Room temperature structure for $Nd_{1/3}NbO_3$ and $Pr_{1/3}NbO_3$

A selection, $1.85<d<2.45$ Å, of the neutron diffraction pattern recorded from $Nd_{1/3}NbO_3$ at room temperature is shown in Fig. 1. The peaks in the figure are identified by indices based on the $2\times2\times2$ cell. Peaks with all even indices correspond to peaks from the ideal cubic aristotype. The superlattice peaks are also indexed on the basis of the $2\times2\times2$ cell, and marked as X-point (two even, one odd indices), R-point (all odd indices), or M-point (one even, two odd indices). Intensities at the X-points arise from A-site cation/vacancy ordering, and those at the R-points from out-of-phase (−) octahedral tilting. The very weak intensities at the M-points are due to X- and R-point distortions acting in concert [15]. Based on the arguments presented by Zhang et al. [13], the most likely structure for $Nd_{1/3}NbO_3$ is either orthorhombic in space group $Cmmm$

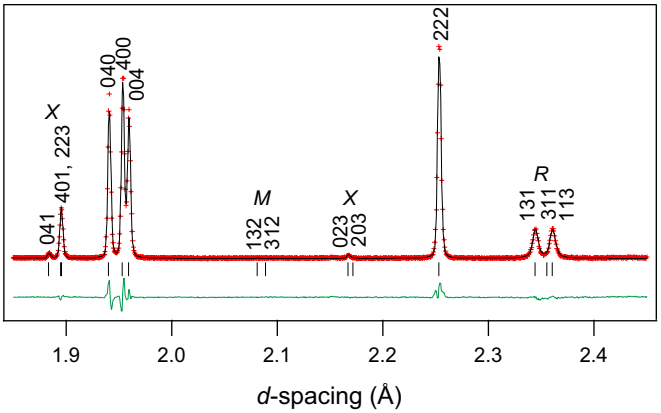

Fig. 1. Extract ($1.85<d<2.45$ Å) from the neutron diffraction pattern recorded in the back-scattering detectors from $Nd_{1/3}NbO_3$ at room temperature. The peaks are indexed on a cell of dimensions $2\times2\times2$ (referred to edge of the cubic aristotype). Crosses represent the observed data. The continuous lines are fits obtained by the Rietveld method using the proposed structure in $Cmmm$, the vertical marks show the peak positions expected in this structure, and the line beneath the pattern records the difference between the observed pattern and that calculated in the Rietveld analysis.

or monoclinic in $C2/m$, both on a $2\times2\times2$ cell. The only difference between these two structures is the number of out-of-phase (−) tilts involved — one tilt (around the a-axis) in $Cmmm$ ($a^-b^0c^0$) but two in $C2/m$ ($a^-b^0c^-$) (around the a- and c-axis), resulting in some very subtle differences in the corresponding diffraction patterns. The most obvious difference lies in the details of the R-point reflections, e.g., the 131/311/113 region would have two roughly equal 131 and 113 peaks but no intensity at 311 in $Cmmm$ [i.e., $I(131)\approx I(113)$ but $I(311)\approx0$], whereas the structure in $C2/m$ would produce intensities at all three reflections [$I(131)>I(113)>I(311)$] [13]. The 131/311/113 region for $Nd_{1/3}NbO_3$, as displayed in Fig. 1, shows two peaks of equal intensity, so clearly indicating that the room temperature structure of $Nd_{1/3}NbO_3$ is orthorhombic in space group $Cmmm$. This is the same structure as proposed previously for $La_{1/3}NbO_3$ [8–10]. It is worthwhile mentioning that the R-point superlattice peaks are broader than the main perovskite peaks and the X-point superlattice reflections. Recalling that the R-point superlattice reflections arise from out-of-phase tilting of the NbO_6 octahedra, we attribute this broadening to the occasional reversal of the sense of this tilt (i.e., the tilting of octahedra in the next plane along the tilting axis is occasionally in the same sense, rather than in the opposite sense as required for out-of-phase tilting). This could occur within an otherwise unaltered framework and so not impact on the other peaks. In other words, we believe this to be kind of a (domain) size broadening, reflecting that the coherence of the out-of-phase octahedral tilting is maintained over only a rather limited range.

Based on the diffraction pattern of $Pr_{1/3}NbO_3$, which is similar to that of $Nd_{1/3}NbO_3$, we conclude that its room temperature structure is also orthorhombic in space group $Cmmm$. Given that $Nd_{1/3}NbO_3$ (this work) and $La_{1/3}NbO_3$ [10] have been shown to be orthorhombic in $Cmmm$, and that the ionic radius of Pr^{3+} is intermediate between those of Nd^{3+} and La^{3+}, this result is to be expected. Our proposed structure in $Cmmm$ for both $Nd_{1/3}NbO_3$ and $Pr_{1/3}NbO_3$ at room temperature differs, however, from the previously reported structure in $Pmmm$ (on a $1\times1\times2$ cell) for these two compounds [4]. Since the observed R-point reflections cannot be indexed on a $1\times1\times2$ cell, the previously proposed structure in $Pmmm$ can definitely be ruled out as the correct structure for these materials.

The room temperature diffraction patterns of $Nd_{1/3}NbO_3$ and $Pr_{1/3}NbO_3$ were fitted, and both lattice parameters and atomic co-ordinates were determined using the Rietveld method [16] as implemented in the GSAS computer program [17,18]. Patterns from both the back-scattering and the 90° detector banks were fitted simultaneously, the diffractometer constant for the 90° bank being released to ensure that the lattice parameters were determined by the higher resolution back-scattering bank. The peak shapes were modelled as convolutions of exponentials with a pseudo-Voigt in which two peak width parameters were varied, and the background as Chebyshev polynomials [17]. Internal co-ordinates were refined along with displacement parameters, and the oxygen displacement parameters were taken to be anisotropic. The distribution of the Nd^{3+}/Pr^{3+} ions over the two crystallographically distinct A-sites was initially allowed to vary, with the sum of the two occupancies being constrained to 2/3 to give an average A-site occupancy of 1/3 as required by the stoichiometry. However, the refinements showed that the A-site at $z=0.5$ is practically empty with a very large uncertainty associated with the corresponding x parameter. Therefore, in the final refinements the Nd (or Pr) occupancies were fixed as 2/3 and 0 at $z=0$ and 0.5, respectively. The broadened R-point reflections were fitted with larger peak widths than the rest of the peaks using the 'stacking fault' model within the GSAS computer program [17]; use of this model improved the goodness of fit significantly (e.g., χ^2 decreasing from 6.0 to 3.5 for $Nd_{1/3}NbO_3$ at room temperature). Details of the room temperature orthorhombic structure in $Cmmm$ for both $Nd_{1/3}NbO_3$ and $Pr_{1/3}NbO_3$ are included in Table 1.

From the atomic coordinates we can estimate the out-of-phase tilt angle of the NbO_6 octahedra around the [100] axis for the orthorhombic structure in space group $Cmmm$: $\phi=1/2\{\tan^{-1}2[y(O1)-y(O2)]+\tan^{-1}2[z(O4)-z(O3)]\}$ [19]. The magnitude of the tilting at room temperature is 8.5° and 8.0° for $Nd_{1/3}NbO_3$ and $Pr_{1/3}NbO_3$, respectively. The slightly larger cell dimensions and smaller tilt angle for $Pr_{1/3}NbO_3$ are as expected from the fact that the Pr^{3+} ions are slightly larger than the Nd^{3+} ions.

It is interesting to note that $Nd_{1/3}NbO_3$ has a higher symmetry than $Nd_{2/3}TiO_3$ (which is believed to be isostructural to $Nd_{0.7}Ti_{0.9}Al_{0.1}O_3$ having a monoclinic structure in $C2/m$) [13], suggesting that the Goldschmidt tolerance factor t {$t=(R_A+R_O)/[\sqrt{2}(R_B+R_O)]$, where R_A, R_B and R_O are the ionic radii of the A- and B-site ions and the O ion, respectively [20]} for $Nd_{1/3}NbO_3$ should be higher than that for $Nd_{2/3}TiO_3$. However, if the presence of vacancies is ignored when applying the formula $t=(R_A+R_O)/[\sqrt{2}(R_B+R_O)]$, the Goldschmidt tolerance factor t would be lower for $Nd_{1/3}NbO_3$ due to the larger ionic radius of Nb^{5+} (0.64 Å) than Ti^{4+} (0.605 Å). The anomaly is resolved by taking the A-site vacancies into account, with an effective size of the vacancy bigger than the ionic radius of Nd^{3+} (1.27 Å).

3.2. Variable temperature studies for $Nd_{1/3}NbO_3$

3.2.1. Low temperature

A consideration of ionic sizes of Nd^{3+} and Pr^{3+} suggests that $Nd_{1/3}NbO_3$ would be the compound more likely to show the lower $C2/m$ symmetry, if not at room temperature, then at low temperatures. We recorded a pattern at 2 K in order to check this possibility. The diffraction pattern was however well fitted assuming the same $Cmmm$ structure as occurs at room temperature, with lattice

Table 1
Refined lattice parameters, Wyckoff sites, fractional atomic coordinates, occupancies and displacement parameters (10^{-2} Å^2) for $Nd_{1/3}NbO_3$ and $Pr_{1/3}NbO_3$ at room temperature, and for $Nd_{1/3}NbO_3$ at 750 °C. The number in parentheses beside each entry indicates the estimated standard deviation referred to the last digit shown

Atom	Site	x	y	z	Occupancy	U_{iso}/U^{11}	U^{22}	U^{33}	U^{12}	U^{13}	U^{23}
$Nd_{1/3}NbO_3$, room temperature: *Cmmm*, $a = 7.8142(1)$, $b = 7.7618(1)$, $c = 7.8369(1)$ Å, $R_{wp} = 4.51\%$, $R_p = 4.29\%$											
Nd	4*g*	0.2557(4)	0	0	0.6667	0.94(3)					
Nb	8*n*	0	0.2494(3)	0.2605(1)	1	1.70(2)					
O1	4*i*	0	0.2889(3)	0	1	3.80(14)	2.47(18)	0.78(9)	0	0	0
O2	4*j*	0	0.2124(3)	0.5	1	3.21(13)	1.50(16)	1.88(10)	0	0	0
O3	4*k*	0	0	0.1994(2)	1	1.34(14)	0.61(14)	1.95(10)	0	0	0
O4	4*l*	0	0.5	0.2722(2)	1	4.69(19)	1.52(15)	1.18(10)	0	0	0
O5	8*m*	0.25	0.25	0.2309(2)	1	1.35(6)	2.66(7)	3.85(8)	−1.45(13)	0	0
$Pr_{1/3}NbO_3$, room temperature: *Cmmm*, $a = 7.8264(1)$, $b = 7.7767(1)$, $c = 7.8554(1)$ Å, $R_{wp} = 4.86\%$, $R_p = 4.57\%$											
Pr	4*g*	0.2555(5)	0	0	0.6667	1.63(5)					
Nb	8*n*	0	0.2499(3)	0.2610(1)	1	2.10(2)					
O1	4*i*	0	0.2864(3)	0	1	3.58(13)	3.00(17)	1.12(8)	0	0	0
O2	4*j*	0	0.2142(3)	0.5	1	3.03(12)	1.83(15)	2.27(8)	0	0	0
O3	4*k*	0	0	0.2016(2)	1	1.54(15)	1.13(14)	2.33(9)	0	0	0
O4	4*l*	0	0.5	0.2698(2)	1	4.41(18)	1.76(14)	1.69(9)	0	0	0
O5	8*m*	0.25	0.25	0.2322(2)	1	1.66(5)	2.68(6)	3.57(7)	−0.75(13)	0	0
$Nd_{1/3}NbO_3$, 750 °C: *P*4/*mmm*, $a = b = 3.9129(1)$, $c = 7.9063(2)$ Å, $R_{wp} = 9.32\%$, $R_p = 7.86\%$											
Nd	1*c*	0.5	0.5	0	0.6667	3.30(10)					
Nb	2*g*	0	0	0.2616(4)	1	3.31(6)					
O1	1*a*	0	0	0	1	7.96(22)	7.96(22)	2.48(27)	0	0	0
O2	1*b*	0	0	0.5	1	7.51(21)	7.51(21)	3.74(27)	0	0	0
O3	4*i*	0	0.5	0.2340(4)	1	6.40(13)	2.73(11)	7.39(14)	0	0	0

Note: Refinements showed that no Nd (or Pr) occupied the *A*-site at $z = 0.5$ in either the orthorhombic (4*h* site in *Cmmm*) or tetragonal (1*d* site in *P*4/*mmm*) structure.

parameters $a = 7.8043(1)$, $b = 7.7534(1)$, $c = 7.8272(1)$ Å and the octahedral tilt angle at 8.8°.

3.2.2. Higher temperatures

High temperature neutron diffraction patterns were recorded from $Nd_{1/3}NbO_3$ in furnace from 100 to 750 °C. As expected, both the magnitude of the orthorhombic splitting (or broadening where not resolved) and the intensity of the *R*-point reflections decrease with increasing temperature. Upon close inspection of the 040/400/004 group of peaks, it appears that the structure is tetragonal at 660 °C [Fig. 2(a)], which is consistent with the transition temperature obtained by strain analysis (see Fig. 4 below). It should be mentioned that, when using neutron diffraction, monitoring the intensity of the *R*-point superlattice reflections is, in general, a more reliable way to determine the transition temperature for continuous phase transitions, as the splitting/broadening of the main perovskite peaks would disappear at a temperature below the actual transition due to limited instrument resolution. In this case, however, it is less accurate to monitor the intensity of the *R*-point reflections as they "collapsed" suddenly at 600 °C as shown in Fig. 2(b). This sudden change is attributed to the onset of extensive local disorder associated with and/or impacting on the octahedral tilting. This may be the result of increased mobility of ions at temperatures somewhat below the temperature of the phase transition.

Structure refinements were carried out for all temperature runs using the same protocol as described earlier. The only difference is that the oxygen displacement parameters were taken to be isotropic in the temperature range of 600–640 °C, where, as shown just above, the *R*-point reflections were extremely broad and weak. Diffraction patterns obtained at 660 °C and above were refined using the tetragonal structure model in *P*4/*mmm*. Again the distribution of Nd^{3+} ions over the two crystallographically distinct *A*-sites was allowed to vary initially, and again the *A*-site at $z = 0.5$ was found to be empty. Accordingly, the Nd occupancies were fixed as 2/3 and 0 at $z = 0$ and 0.5, respectively in the final refinements. Details of the tetragonal structure in *P*4/*mmm* at 750 °C are included in Table 1.

Fig. 3 shows the temperature dependence of the lattice parameters obtained from refinements, this indicating that the orthorhombic to tetragonal phase transition is continuous. From the lattice parameters we can also derive the spontaneous strains, with the symmetry-breaking strain as $e_{ortho} = e_1 - e_2 = (a-b)/a_0$, where a_0 is the lattice parameter in the absence of the phase transition, estimated in this context using $a_0 \approx (a+b)/2$. This strain has a symmetry[2]

[2]That is the orthorhombic strain e_{ortho} transforms under the operations of the parent space group *P*4/*mmm* in a manner determined by the matrices of its irreducible representation Γ_2^+ (notation of Miller and Love [21]).

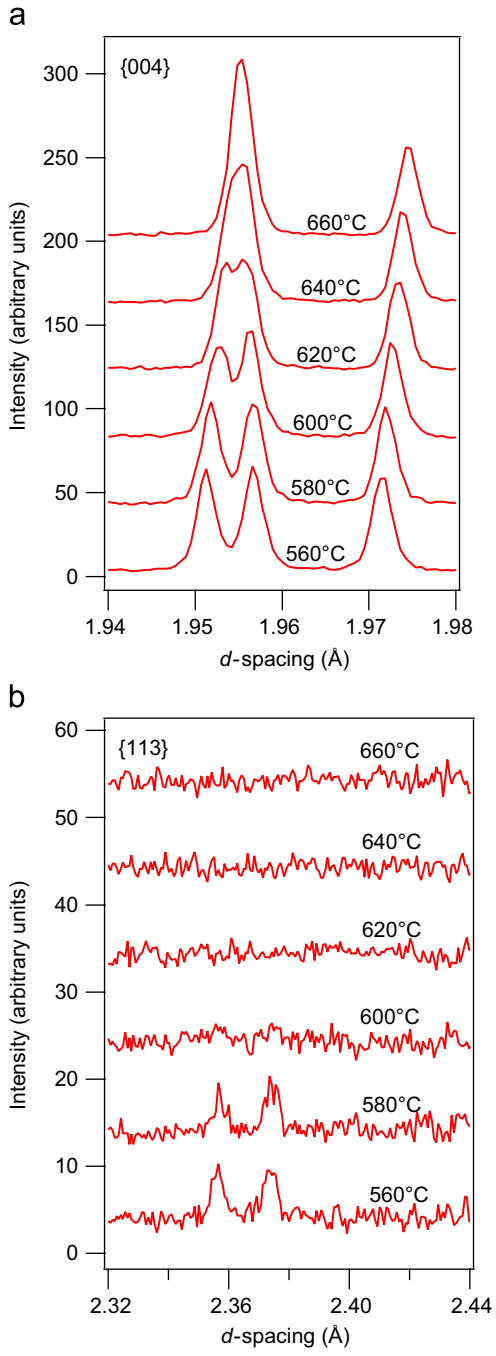

Fig. 2. Extracts from the neutron diffraction patterns of $Nd_{1/3}NbO_3$ as recorded in the back-scattering detector bank: (a) $1.94 < d < 1.98$ Å, and (b) $2.32 < d < 2.44$ Å, showing the evolution of the {004} and {113} (*R*-point) reflections, respectively, as a function of temperature. The brackets here are intended to refer to a set of reflections that would be equivalent for the cubic perovskite.

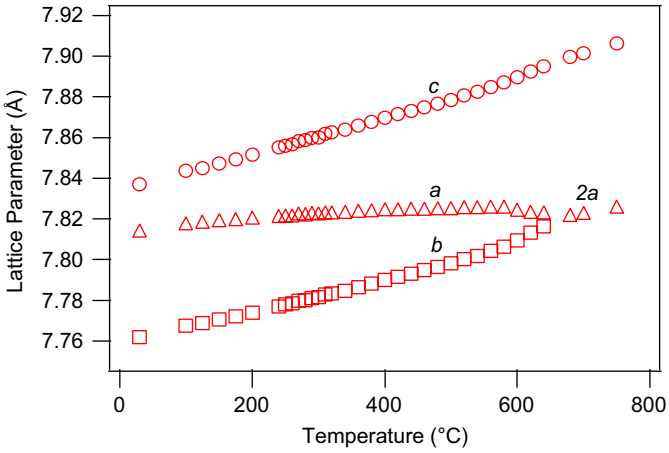

Fig. 3. Lattice parameters for $Nd_{1/3}NbO_3$ as a function of temperature.

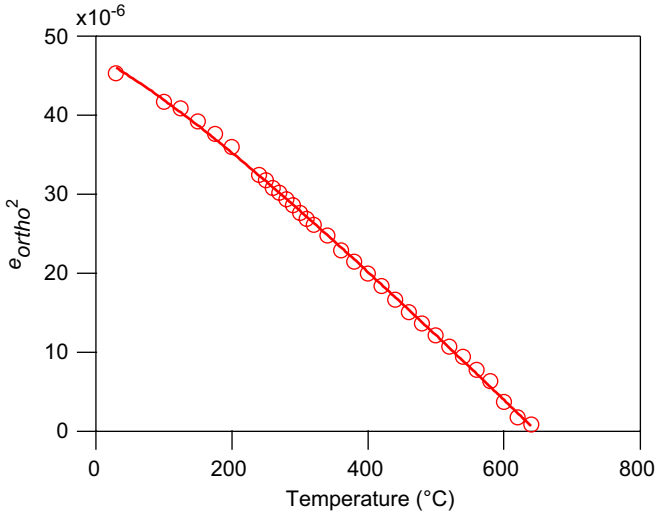

Fig. 4. The temperature dependence of e^2_{ortho}, the square of the orthorhombic strain for $Nd_{1/3}NbO_3$. The fitted curve is of the form $e^2_{\mathrm{ortho}} \propto \Theta_s(\coth(\Theta_s/T_c) - \coth(\Theta_s/T))$, giving $T_c \approx 650\,^{\circ}\mathrm{C}$ and $\Theta_s \approx 115\,^{\circ}\mathrm{C}$.

(Γ_2^+) that differs from that (M_5^-) of the thermodynamic order parameter Q for the octahedral tilting transition, so we expect e_{ortho} to be proportional to Q^2 [22,23]. As can be seen in Fig. 4, the square of the orthorhombic strain varies with temperature in a practically linear fashion, implying $Q^4 \propto T_c - T$, hence a transition tricritical in nature [22].

The fitted curve in Fig. 4 is in fact of the form

$$e^2_{\mathrm{ortho}} \propto \Theta_s(\coth(\Theta_s/T_c) - \coth(\Theta_s/T)),$$

to account for saturation effects at lower temperatures. The T, T_c and Θ_s in the above expression are the temperature, transition temperature and saturation temperature, respectively, expressed in degrees Kelvin. Based on this fit the transition temperature is estimated as $T_c \approx 650\,^{\circ}\mathrm{C}$.

To the extent that the octahedral tilt angle ϕ represents the order parameter, we would expect e_{ortho} to be proportional to ϕ^2 (i.e., ϕ^4 would then show the same temperature dependence as e^2_{ortho}). Fig. 5 shows a plot of ϕ^2 against e_{ortho} using data up to 580 °C — one consequence of the "collapse" of the *R*-point reflections was that tilt angles at $580\,^{\circ}\mathrm{C} < T < T_c$ could not be estimated with any confidence. It can be seen in Fig. 5 that the relationship between ϕ^2 and e_{ortho} appears to be linear, but the line does not pass through the origin. This means that the tilt angle is

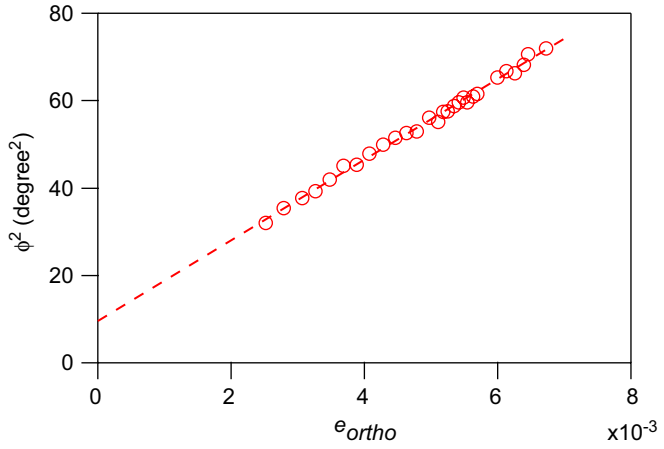

Fig. 5. Relationship between the orthorhombic strain, e_{ortho}, and the square of the octahedral tilt angle ϕ, usually taken to represent the order parameter for the transition in $Nd_{1/3}NbO_3$.

not zero at the transition temperature derived from the strain analysis (or the transition temperature extrapolated from the tilt angle would be at a higher temperature). Such deviation from direct proportionality has been reported previously for the ordered double perovskites $Ba_2Bi_2O_6$ and Ba_2BiSbO_6 [24], and even for the "classic" second order transition in the simple perovskite $LaAlO_3$ (Fig. 10 in Ref. [25]). The deviation has been attributed to an average angle of dynamical tilting at the transition in the former case or changes in domain wall mobility in the latter case. Given that the lattice parameters (from which the strain is derived) are determined more precisely than the oxygen coordinates (which define the tilt angle), we suggest that the far more reliable estimate of the transition temperature would be that from the strain.

4. Conclusions

We have determined the crystal structure of $Nd_{1/3}NbO_3$ and $Pr_{1/3}NbO_3$ as orthorhombic in space group *Cmmm* at room temperature, using high-resolution neutron powder diffraction. The orthorhombic distortion results from *A*-site cation/vacancy ordering and tilting of the NbO_6 octahedra. It has been shown that $Nd_{1/3}NbO_3$ maintains the same structure down to 2 K, and it can be presumed on the basis of ionic sizes that $Pr_{1/3}NbO_3$ would maintain this structure too.

We have also examined the phase transition behaviour of $Nd_{1/3}NbO_3$. Upon heating, $Nd_{1/3}NbO_3$ undergoes a continuous transformation to tetragonal structure in *P4/mmm* near 650 °C, as a consequence of the progressive removal of the octahedral tilting. The temperature dependence of the strain is consistent with a tricritical phase transition. $Pr_{1/3}NbO_3$ is expected to undergo a similar phase transition at a slightly lower temperature.

Acknowledgments

We acknowledge the travel support to ISIS for ZZ and BJK, provided by the Commonwealth of Australia under the Major National Research Facilities Program. This work was partially supported by the Australian Research Council (ARC). The neutron facilities at ISIS are operated by the Council for the Central Laboratory of the Research Councils (CCLRC), with a contribution from the ARC. We are also grateful to Prof. Michael Carpenter at University of Cambridge for his advice on strain analysis.

References

[1] A. Nadiri, G. Le Flem, C. Delmas, J. Solid State Chem. 73 (1988) 338–347.
[2] M. Nakayama, M. Wakihara, Y. Kobayashi, H. Miyashiro, J. Phys. Chem. B 109 (2005) 14648–14653.
[3] E. Orgaz, A. Huanosta, J. Solid State Chem. 97 (1992) 65–73.
[4] A.M. Abakumov, R.V. Shpanchenko, E.V. Antipov, Mat. Res. Bull. 30 (1995) 97–103.
[5] S. Ebisu, T. Sogabe, M. Hayashi, S. Nagata, J. Phys. Chem. Solids 61 (2000) 869–874.
[6] P.N. Iyer, A.J. Smith, Acta Crystallogr. 23 (1967) 740–746.
[7] C. Bridges, J.E. Greedan, J. Barbier, Acta Crystallogr. B 56 (2000) 183–188.
[8] R.A. Dilanian, A. Yamamoto, F. Izumi, T. Kamiyama, Mol. Cryst. Liq. Cryst. 341 (2000) 225–230.
[9] L. Carrillo, M.E. Villafuerte-Castrejón, G. González, L.E. Sansores, L. Bucio, J. Duque, R. Pomés, J. Mat. Sci. 35 (2000) 3047–3052. Note: although the correct space group of *Cmmm* was determined from their electron diffraction data, we do not consider the choice of atomic (Wyckoff) positions correct in their proposed structure.
[10] B.J. Kennedy, C.J. Howard, Y. Kubota, K. Kato, J. Solid State Chem. 177 (2004) 4552–4556.
[11] C.J. Howard, Z. Zhang, Acta Crystallogr. B 60 (2004) 249–251; erratum B 60 (2004) 763.
[12] R.D. Shannon, Acta Crystallogr. A 32 (1976) 751–767.
[13] Z. Zhang, C.J. Howard, K.S. Knight, G.R. Lumpkin, Acta Crystallogr. B 62 (2006) 60–67.
[14] R.M. Ibberson, W.I.F. David, K.S. Knight, *Rutherford Appleton Laboratory Report* RAL92-031, 1992.
[15] D.I. Woodward, I.M. Reaney, Acta Crystallogr. B 61 (2005) 387–399.
[16] H.M. Rietveld, J. Appl. Crystallogr. 2 (1969) 65–71.
[17] A.C. Larson, R.B. von Dreele, General Structure Analysis System (GSAS), Los Alamos National Laboratory Report LAUR 86-748, 2000.
[18] B.H. Toby, J. Appl. Crystallogr. 34 (2001) 210–213.
[19] C.J. Howard, Z. Zhang, J. Phys.: Condens. Matter 15 (2003) 4543–4553.
[20] R.S. Roth, J. Res. Natl. Bur. Std. 58 (1957) 75–88.
[21] S.C. Miller. W.F. Love, Tables of Irreducible Representations of Space Groups and Co-Representations of Magnetic Space Groups, Preutt Press, Boulder, CO, 1967.
[22] E.K.H. Salje, Phase Transitions in Ferroelastic and Co-Elastic Crystals, Cambridge University Press, Cambridge, 1990.
[23] M.A. Carpenter, E.K.H. Salje, A. Graeme-Barber, Eur. J. Mineral. 10 (1998) 621–691.
[24] B.J. Kennedy, C.J. Howard, K.S. Knight, Z. Zhang, Q. Zhou, Acta Crystallogr. B 62 (2006) 537–546.
[25] S.A. Hayward, F.D. Morrison, S.A.T. Redfern, E.K.H. Salje, J.F. Scott, K.S. Knight, S. Tarantino, A.M. Glazer, V. Shuveava, P. Daniel, M. Zhang, M.A. Carpenter, Phys. Rev. B 72 (2005) 054110.